U.S. DEPARTMENT OF ENERGY

PNNL-36560

Prepared for the U.S. Department of Energy
under Contract DE-AC05-76RL01830

Effects of irradiation temperature on the microstructure and deuterium retention in γ-$LiAlO_2$ pellets

Weilin Jiang
Andrew M. Casella
David J. Senor

Final Report
Tritium Modernization Program
September 2024

Pacific Northwest
NATIONAL LABORATORY

Proudly Operated by Battelle *Since 1965*

Effects of irradiation temperature on the microstructure and deuterium retention in γ-$LiAlO_2$ pellets

Weilin Jiang, Andrew M. Casella, David J. Senor
PNNL Contributors: Karen Kruska, Zihua Zhu
Texas A&M University Contributors: Zhihan Hu, Lin Shao

Summary

This report presents the experimental findings obtained from November 2023 to September 2024. The study aims to investigate the effects of temperature on the microstructure, deuterium (D) retention, and lithium (Li) loss in γ-$LiAlO_2$ pellets subjected to sequential He^+ and D^+ ion irradiation to a high dose. Sequential ion irradiation has been a key method in our previous studies to simulate the behavior of γ-$LiAlO_2$ under neutron irradiation. In addition to dose and dose rate, irradiation temperature is a critical factor influencing microstructural and compositional changes. $LiAl_5O_8$ precipitates have been observed in γ-$LiAlO_2$ pellets irradiated with reactor neutrons at ~300°C. These precipitates also form during ion irradiation at an elevated temperature of 500°C, but not at 300°C. In our ion irradiation experiments, the dose rate is typically three orders of magnitude higher than that of neutron irradiation, leading to a more rapid damage production. To better emulate the microstructural features in neutron-irradiated pellets using ion irradiation, a higher irradiation temperature is needed to accelerate the diffusion of point defects and enhance defect recovery rates, thereby compensating for the effects of the higher dose rate. The microstructural changes observed are the result of competing processes occurring during ion irradiation.

Our previous studies revealed a marked difference in the microstructure and lithium loss of γ-$LiAlO_2$ pellets subjected to sequential He^+ and D^+ ion irradiation at 300°C and 500°C. Irradiation temperature was found to significantly affect deuterium retention and lithium loss, with implications for tritium behavior as well. However, data at intermediate temperatures between 300°C and 500°C have been lacking. In this study, we explore the effects of sequential irradiation on γ-$LiAlO_2$ pellets at 350°C, 400°C, 450°C, and 500°C using 120 keV He^+ and 80 keV D_2^+ ions. The ion fluence was maintained at 3×10^{17} $(He^+ + D^+)/cm^2$ across all temperatures, with ion fluxes of 3×10^{13} $(He^+/cm^2)/s$ and 2.5×10^{13} $(D^+/cm^2)/s$. The irradiated pellets were subsequently characterized using scanning transmission electron microscopy (STEM) and time-of-flight secondary ion mass spectrometry (ToF-SIMS).

The results of this study indicate that at 350°C, no precipitates were observed, but the microstructures exhibited cavities and fractures. At 400°C, small precipitates began to form in the irradiated region, accompanied by surface amorphization, fractures, and cavities. These observations suggest that the critical temperature for precipitate formation under the given ion irradiation conditions lies between 350°C and 400°C. At 450°C, faceted precipitates and cavities were present, along with an amorphized surface. As the temperature increased to 500°C, larger faceted precipitates developed, and surface amorphization persisted. Moreover, significant lithium loss and isotope exchange between environmental hydrogen and implanted deuterium were detected during ion irradiation at 500°C. At the typical ion flux of 3×10^{13} $(ions/cm^2)/s$, sequential irradiation with He^+ and D^+ ions at 500°C is recommended to emulate the microstructural features in γ-$LiAlO_2$ irradiated with a thermalized fission neutron spectrum at ~300°C.

Table of Contents

1. Introduction

Sequential irradiation of γ-$LiAlO_2$ pellets with He^+ and D_2^+ ions has been extensively applied in our previous studies [1-5] to emulate the response of γ-$LiAlO_2$ pellets to neutron irradiation, using deuterium ions as a surrogate for tritium particles. This approach has successfully reproduced the major microstructural features and gas transport behavior observed in neutron-irradiated pellets. Besides dose and dose rate, irradiation temperature is also a critical parameter that dictates the microstructural and compositional changes. $LiAl_5O_8$ precipitates are observed in γ-$LiAlO_2$ pellets irradiated with a thermalized fission neutron spectrum at ~300°C [5], as shown in Figure 1(a). However, these precipitates do not appear during sequential irradiation with He^+ and D_2^+ ions at the same temperature [4], as shown in Figure 1(b). At 500°C, precipitates form in the microstructure [4,5], as exhibited in Figure 1(c). Further investigations of the microstructure show that ion irradiation of γ-$LiAlO_2$ pellets at 500°C reproduces the major features from neutron irradiation, such as precipitates surrounded by cavities [1], denuded zones around the grain boundaries [5], and aggregation of cavities on some grain boundaries [5]. In addition, the precipitate crystal structure has been determined to be spinel-like, with the same lattice parameter as $LiAl_5O_8$ and γ-Al_2O_3 [5,6]. The precipitate compositions have been measured, showing that they contain Li with concentrations varying by location. The results suggest that theses precipitates are not a perfect, but rather non-stoichiometric $LiAl_5O_8$ crystal [5]. From Figure 1, the precipitate size resulting from ion irradiation at 500°C is one to two orders of magnitude smaller than that observed from neutron irradiation to a similar dose at ~300°C.

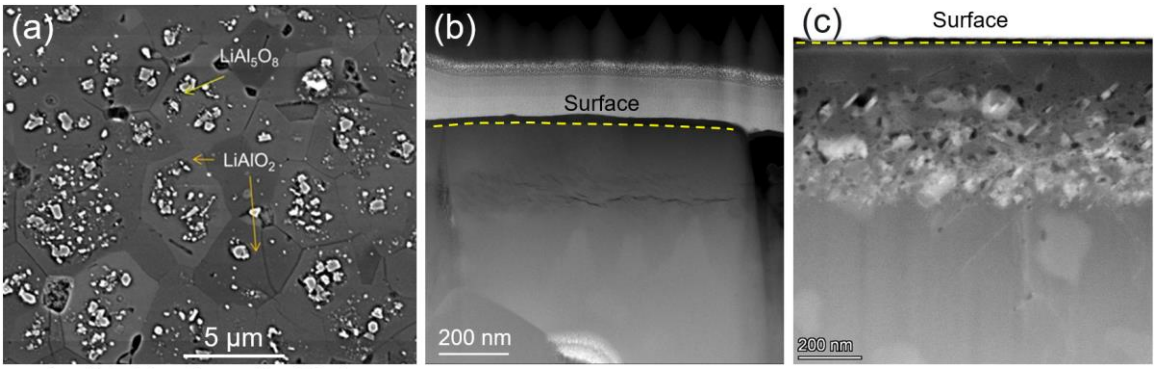

Figure 1. Microstructures of γ-$LiAlO_2$ pellets irradiated with (a) neutrons at ~300°C, (b) He^+ and D_2^+ ions at 300°C, and (c) He^+ and D_2^+ ions at 500°C.

Typically, the dose rate for ion irradiation is several orders of magnitude higher than that for neutron irradiation [7]. High-dose rates could lead to formation of more complex defects in the pellets during irradiation. Presence of these defects could create deeper trapping sites for migrating atoms, including Li and gas species. Consequently, a higher temperature may be required to detrap these atoms during atomic diffusion, microstructural evolution, and elemental redistribution. In addition to a sharp contrast in the microstructure of γ-$LiAlO_2$ pellets sequentially irradiated with He^+ and D^+ ions at 300°C and 500°C as reported from our previous studies [4,8], a significant impact of irradiation temperature on deuterium (and by inference, tritium) retention was also observed [3]. Recently, we completed a tritium science study of

structural and compositional evolutions in γ-$LiAlO_2$ pellets as a function of dose during ion irradiation [5]. To fill the knowledge gap and determine the temperature shift for better application of ion irradiation to emulate neutron irradiation effects, we have performed a systematic study of irradiation temperature effects in γ-$LiAlO_2$ pellets. The results from this study are expected to provide a clearer picture of the microstructural evolution, D retention, and compositional changes controlled by the two correlated irradiation parameters: dose and temperature.

2. Experimental Details

2.1 SRIM simulation

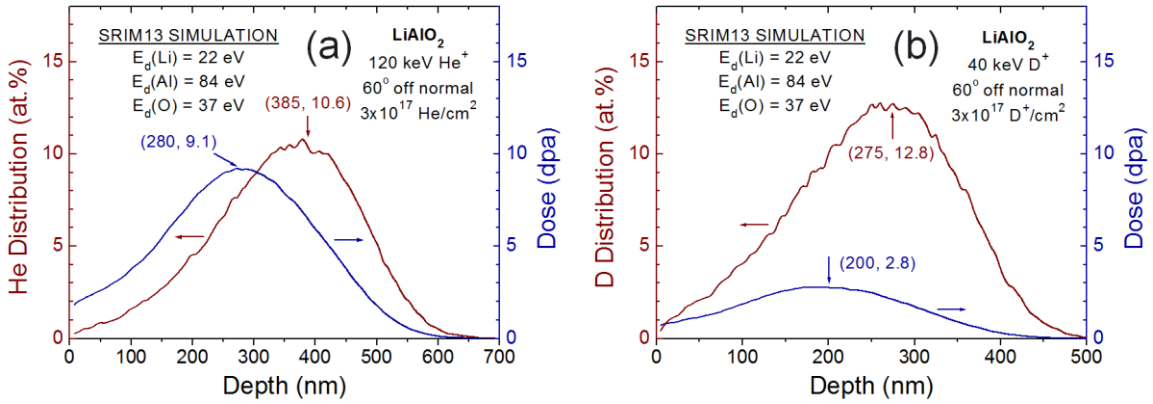

Figure 2. Depth profiles of the atomic percentages and doses from SRIM13 simulations for (a) 120 keV He^+ and (b) 40 keV D^+ ion irradiations of γ-$LiAlO_2$ at 60° off normal to a fluence of 3×10^{17} ions/cm^2.

Table 1. Sequential ion irradiation of γ-$LiAlO_2$ to a fluence of 3×10^{17} (He^++D^+)/cm^2 at a tilted angle of 60° and SRIM13 simulation results.

Sample ID	Ion Beam	Temperature (°C)	Damage Peak (nm)	Dose (dpa)	Concentration Peak (nm)	Concentration (at.% He or D)
S350C	120 keV He^+ 80 keV D_2^+	350	280 200	9.1 2.8	385 275	10.6 12.8
S400C	120 keV He^+ 80 keV D_2^+	400	280 200	9.1 2.8	385 275	10.6 12.8
S450C	120 keV He^+ 80 keV D_2^+	450	280 200	9.1 2.8	385 275	10.6 12.8
S500C	120 keV He^+ 80 keV D_2^+	500	280 200	9.1 2.8	385 275	10.6 12.8

3×10^{17} (He^++D^+)/cm^2 corresponds to ~19 at.% ^{6}Li burnup in γ-$^6LiAlO_2$ irradiated with a thermalized fission neutron spectrum at ~300°C [3].

As discussed previously [5], thermal neutron irradiation of γ-$LiAlO_2$ pellets can be emulated by irradiation with both 2.05 MeV He^+ and 2.75 MeV T^+ ions to an equal ion fluence in terms of irradiation

damage generation. Both ions initially dissipate their energies predominantly through electronic processes in the γ-$LiAlO_2$ pellets. Below 15 and 25 keV/amu, the nuclear stopping powers of T^+ and He^+ ions, which are responsible for producing lattice damage in γ-$LiAlO_2$, become increasingly significant, with their highest nuclear stopping powers occurring at 0.225 and 0.5 keV, respectively. In our emulation of neutron irradiation, we have used D^+ ions as a surrogate for T^+ ions. Most of the lattice damage is produced by the heavier He^+ ions. To emulate possible trapping of D atoms at the defects produced by He^+ ions, sequential ion irradiation of He^+ and D^+ ions is designed so that the D concentration peak overlaps with the He^+ damage peak. Consistent with our previous studies, SRIM13 (Stopping and Range of Ions in Matter, version 2013) simulation results [9] for irradiation at an incident angle of 60° with 120 keV He^+ ions and 40 keV D^+ ions in γ-$LiAlO_2$ (mass density ρ = 2.615 g/cm^3) are used, which are shown for an ion fluence of 3×10^{17} ions/cm^2 in Figure 2. This ion fluence corresponds to a total ^{6}Li burnup of ~19.2 at.% [3] in γ-$^6LiAlO_2$ pellets irradiated with a thermalized fission neutron spectrum at ~300°C.

Monolayer collision step/surface sputtering mode was chosen to eliminate artifacts into the sample damage caused by energetic light ions in the near-surface region. In the simulation, the threshold displacement energies of E_d(Li) = 22 eV, E_d(Al) = 84 eV and E_d(O) = 37 eV were adopted from a molecular dynamics (MD) simulation [10] and the surface binding energies were set equal to the threshold displacement energies on corresponding sublattices. The peak doses and atomic concentrations of He and D in the pellet from the SRIM13 simulations are listed in Table 1. For He^+ ion irradiation, the peak dose is 9.1 dpa at 280 nm, and the peak He concentration is 10.6 at.% at 385 nm. Similarly, the peak dose for D^+ ion irradiation is 2.8 dpa at 200 nm, and the D peak concentration is 12.8 at.% at 275 nm. Thus, the peak position of the implanted D profile under the irradiation conditions is well overlapped spatially with that of the He damage profile, as desired. It should be noted that a recent report [11] suggests an approach that uses the full-damage cascade option in SRIM13 with manual manipulation of irradiation parameters. In this study, the dose values estimated from SRIM13 simulations are used for relative comparisons, and the absolute dose values do not affect data interpretation.

2.2 Ion irradiation

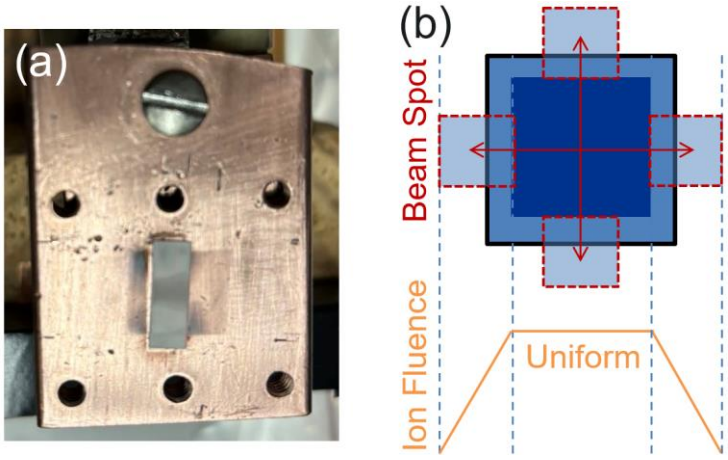

Figure 3. (a) γ-$LiAlO_2$ pallet after sequential ion irradiation at 500°C, and (b) schematic of the beam rastering area on the sample.

Ion irradiation was performed at Texas A&M University using a 140 kV ion accelerator equipped with a magnetic rastering system. Sequential ion irradiation was performed at 60° off the surface normal with 120 keV He^+ ions and 80 keV D_2^+ ions to a fluence of 3×10^{17} $(He^+ + D^+)/cm^2$ at 350°C, 400°C, 450°C and 500°C. The samples are labeled as S350C, S400C, S450C, and S500C, respectively, as detailed in Table 1.

The pellets were first irradiated with He^+ ions to produce defects in a range of depth, followed by implantation with D^+ ions in the same depth region to allow interaction between the damage cascades, D atoms, He atoms, and stabilized defects produced by the He^+ ion irradiation. A D_2^+ molecular beam was chosen instead of a D^+ beam due to its higher ion flux. The 80 keV D_2^+ ions are equivalent to 40 keV D^+ ions for ion irradiation. Low-energy and tilted geometry were employed for convenience of elemental depth profiling. Ion beams were rastered over an area to achieve a more uniform irradiation, as schematically illustrated in Figure 3(b). Irradiation was manually interrupted about every 15 min to check the beam current, which was arithmetically averaged over the period. Despite this procedure, the absolute ion fluence is subject to an error of up to 10% or greater. On average, the He^+ and D_2^+ beam fluxes were 3×10^{13} $He^+/cm^2/s$ and 2.5×10^{13} $D^+/cm^2/s$, respectively. The samples were heated to the desired temperatures using a filament behind the copper sample holder prior to ion irradiation.

2.3 Sample preparation and characterization

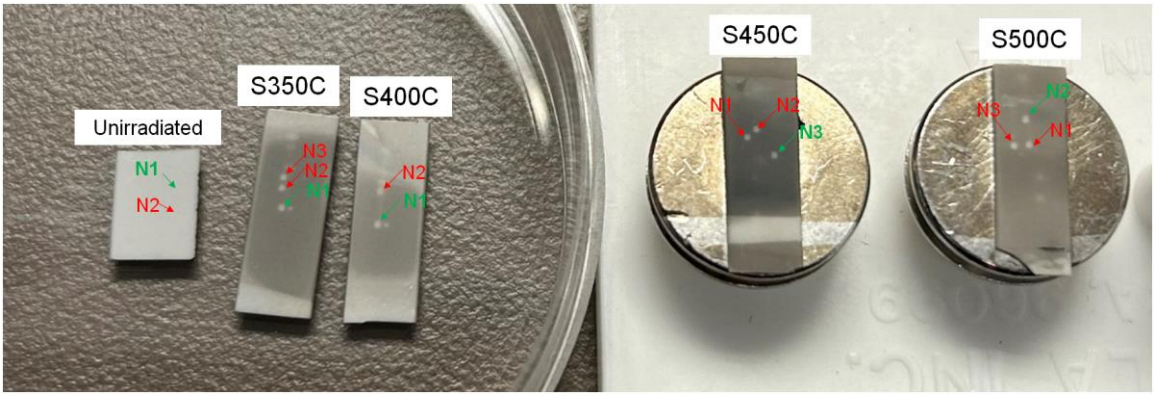

Figure 4. ToF-SIMS analytical spots on γ-$LiAlO_2$ pallets sequentially irradiated with He^+ and D_2^+ ions.

Cross-sectional scanning transmission electron microscopy (STEM) specimens were prepared from a dark area near the center of the irradiated pellet using a FEI Quanta 3D dual-beam focused ion beam (FIB) microscope, as shown in Figure 4. Regions of interest were capped with ~300 nm of electron deposited Pt and 4 μm of ion deposited C to protect the surface during milling and thinning. Lamellae were extracted using a standard lift-out procedure with a Ga^+ ion beam and attached to a Cu grid. A window in the lift-out was thinned starting at a high tilt (±5° from 52°) with the Ga^+ ion beam at 30 kV, reducing the tilt by 1° steps as the beam energy is reduced to 16 kV, 8 kV and 5 kV. When the sample is roughly 100 nm thick, the sample is tilted to 59° (±7° from 52°), and the beam energy reduced to 2 kV for final thinning polish. The FIB samples were examined using a JEOL JEM-ARM 200CF aberration-corrected TEM/STEM microscope operating at 200 kV. High-angle annular dark field (HAADF) STEM was used to image the irradiated materials.

ToF-SIMS measurements were performed at room temperature using TOF.SIMS5 instrument (IONTOF GmbH, Münster, Germany) in dual beam, non-interlaced mode for depth profiling of H, D, Li, C, O and Al in the pellets. Both dark and bright areas due to non-uniformity of ion irradiation were analyzed, with three spots for each of samples S350C, S450C, and S500C, and two spots for S400C. The green-numbered spots, taken in the dark areas, were used for data analysis, as shown in Figure 4. A 2.0 keV Cs^+ beam was used as the sputtering beam, and a 25 keV Bi^+ beam served as the analytical beam. The Cs^+ sputtering beam (~59 nA) was scanned over an area of 200 µm × 200 µm. The pulsed Bi^+ beam, focused to ~5 µm in diameter with a beam current of ~0.75 pA at a frequency of 10 kHz, was rastered over an area of 50 µm × 50 µm at the center of the Cs^+ sputter crater. The non-interlaced mode operated with 10.0 s sputtering, 2.0 s pause, and 3.28 s data collection. A low energy (10 eV) electron flood gun was used for charge compensation.

3. Results and Discussion

3.1 Dependence of microstructural features on irradiation temperature

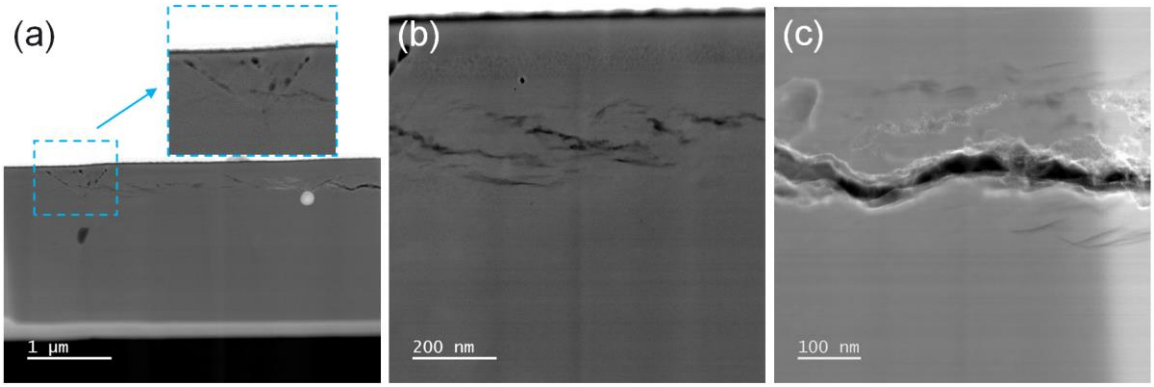

Figure 5. STEM micrographs of the microstructure of a γ-$LiAlO_2$ pallet irradiated at 350°C to 3×10^{17} $(He^+ + D^+)/cm^2$ at (a) low, (b) medium, and (c) high magnifications.

Figure 5 shows HAADF STEM images at various resolutions for the microstructure of a γ-$LiAlO_2$ pellet irradiated to 3×10^{17} $(He^+ + D^+)/cm^2$ at 350°C (S350C). No solid precipitates are observed in the microstructure. Instead, a fracture-like feature emerges around the depth of the He concentration peak, as shown in Figures 5(b) and (c). A similar microstructure was also observed in a γ-$LiAlO_2$ pellet irradiated to 2×10^{17} $(He^+ + D^+)/cm^2$ at 300°C [4]. Cavities appear to aggregate at the gran boundaries, as shown in Figure 5(a). The formation of these cavities is due to the interaction of vacancies with He atoms, likely involving D atoms as well. The bright and dark contrasts seen in Figure 5(a) correspond to the pre-existing particles of ZrO_2 (impurities introduced during the powder milling process) and $LiAl_5O_8$ (a secondary phase), respectively, in the γ-$LiAlO_2$ pellet.

For irradiation to 3×10^{17} $(He^+ + D^+)/cm^2$ at 400°C (S400C), significant microstructural changes are observed, as shown in Figure 6. There appears to be an amorphized surface layer with a thickness of ~70 nm, likely due to radiolysis. A prominent fracture is evident at the depth of the He concentration peak, as shown in Figure 6(a). The wave-like contrast observed is an artifact rather than a feature induced by ion

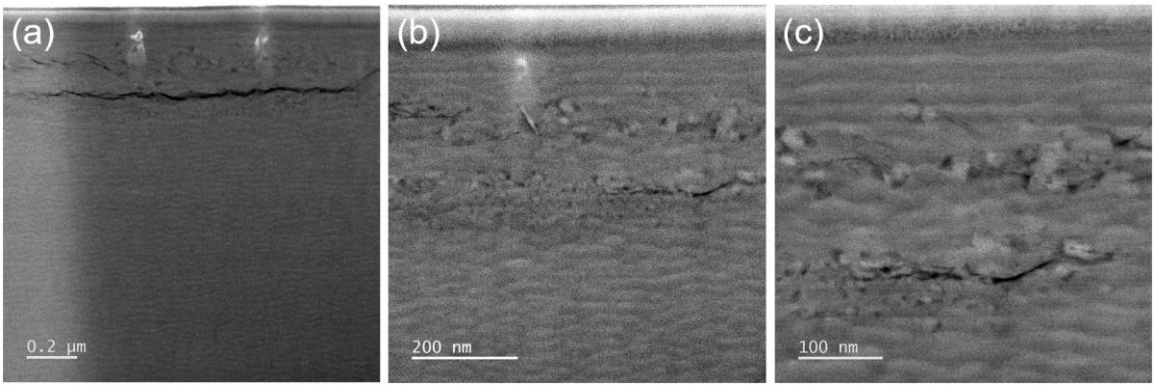

Figure 6. STEM micrographs of the microstructure of a γ-$LiAlO_2$ pallet irradiated at 400°C to 3×10^{17} $(He^+ + D^+)/cm^2$ at (a) low, (b) medium, and (c) high magnifications.

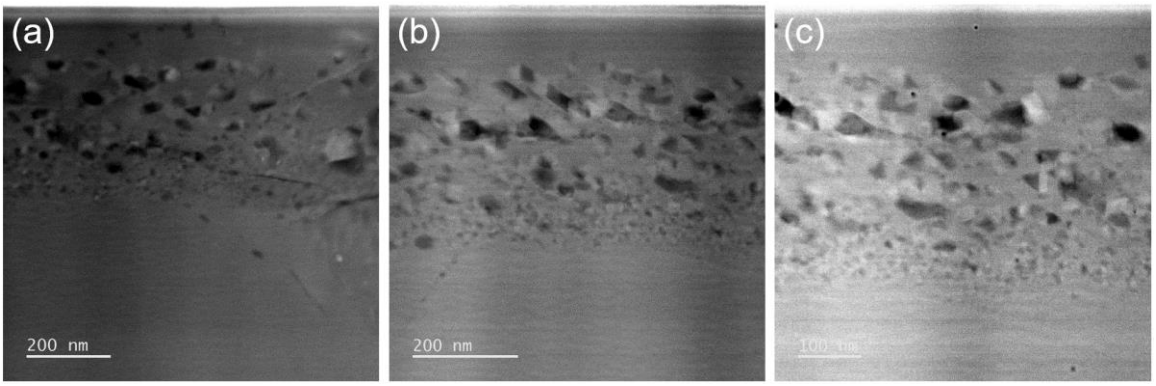

Figure 7. STEM micrographs of the microstructure of a γ-$LiAlO_2$ pallet irradiated at 450°C to 3×10^{17} $(He^+ + D^+)/cm^2$ at (a) low, (b) medium, and (c) high magnifications.

irradiation, as it is also present well beyond the depth of ion irradiation [Figure 6(a)]. From Figure 6, small precipitates and cavities form around the damage peak region, where there are also some apparent fractures. The results indicate that at the given ion flux of this study (3×10^{13} $He^+/cm^2/s$ and 2.5×10^{13} $D^+/cm^2/s$), the critical temperature for precipitate formation lies between 350°C and 400°C.

As the irradiation temperature increases to 450°C (S450C), a surface amorphized layer remains present, as shown in Figure 7. Compared to the precipitates formed at 400°C, those at 450°C grow larger, become faceted, and are distributed in a wider depth region from 120 to 410 nm. This behavior is expected, as higher temperatures accelerate defect migration and increase the growth rate of precipitates. The dark contrast seen in Figure 7(a) represents cavities, which extend to nearly 600 nm. Although small fractures may be present in the irradiated microstructure, no large fractures are observed. The exact reasons for this absence are not yet fully understood. However, it is likely that the faster diffusion of vacancies and gas species plays a significant role. At higher temperatures, increased gas release and enhanced vacancy annihilation during ion irradiation could contribute to this phenomenon.

At 500°C (S500C), a darker amorphized layer is evident beneath the surface protection cap, with a portion of the cap still visible in the upper left corner of the FIB sample, as shown in Figure 8(a). A large, faceted precipitates, ~200 nm in size, is observed near the surface, with a higher density of smaller precipitates distributed around the damage peak. Some of these precipitates are surrounded by cavities,

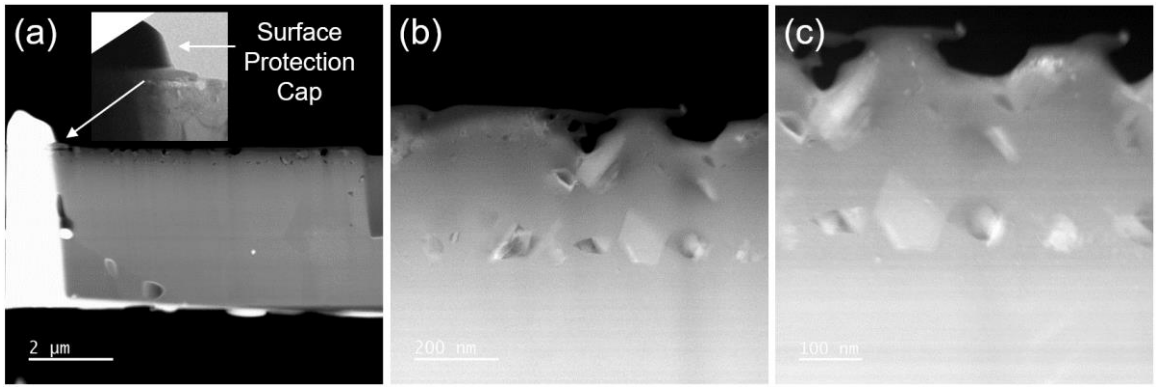

Figure 8. STEM micrographs of the microstructure of a γ-$LiAlO_2$ pallet irradiated at 500°C to 3×10^{17} $(He^+ + D^+)/cm^2$ at (a) low, (b) medium, and (c) high magnifications.

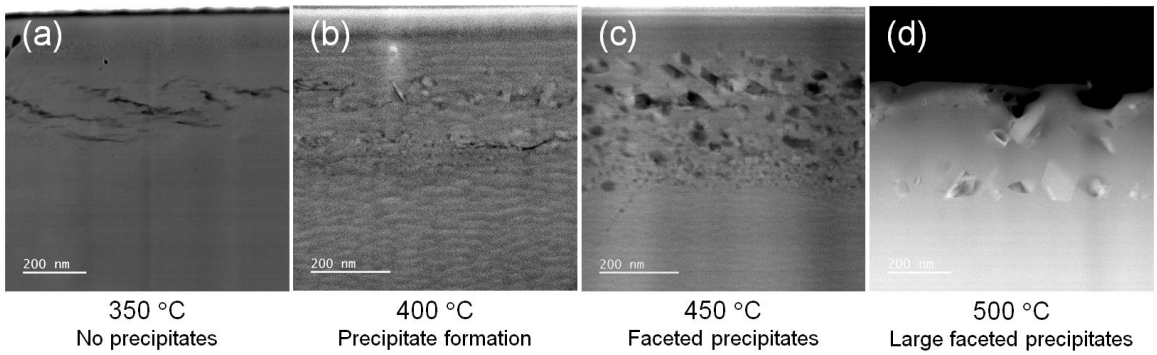

Figure 9. STEM micrographs of the microstructures of γ-$LiAlO_2$ pallets irradiated to 3×10^{17} $(He^+ + D^+)/cm^2$ at (a) 350°C, (b) 400°C, (c) 450°C, and (d) 500°C.

consistent with previous observations [1]. Large cavities, up to 150 nm in size, form near the surface, spanning both amorphized and crystalline regions. Structural fractures at the He concentration peak are absent, likely due to the rapid diffusion of He atoms and vacancies to the surface during ion irradiation at 500°C. This microstructure closely resembles that observed in a γ-$LiAlO_2$ pellet subjected to the same irradiation conditions in a previous study [5].

Figure 9 compares the microstructures of γ-$LiAlO_2$ pellets irradiated to 3×10^{17} $(He^+ + D^+)/cm^2$ at temperatures ranging from 350°C to 500°C. At 350°C, no solid precipitates are observed; instead, the microstructure exhibits cavities and fractures at the He concentration peak. At 400°C, small precipitates begin to appear, along with an amorphized surface layer, structural fractures, and cavities. The critical temperature for precipitate formation under the irradiation conditions of this study lies between 350°C and 400°C. At 450°C, faceted precipitates form, accompanied by cavities and surface amorphization. At 500°C, large, faceted precipitates are developed near the amorphized surface, and a high density of smaller precipitates is observed around the damage peak.

A temperature of 500°C is recommended for sequential He^+ and D^+ ion irradiation at the typical ion flux on the order of 3×10^{13} $(ions/cm^2)/s$ to emulate the microstructural features observed in γ-$LiAlO_2$ irradiated in a thermalized fission neutron spectrum at ~300°C. A higher ion fluence should be applied to increase the concentration of implanted He and D, thereby compensating for the greater gas release at

elevated ion irradiation temperatures. Lower ion flux is expected to result in the formation of larger $LiAl_5O_8$ precipitates, more closely resembling those formed in neutron-irradiated γ-$LiAlO_2$ pellets. Although a similar effect could be anticipated for ion irradiation at higher than 500°C, gas diffusion and release could be more significantly enhanced compared to neutron irradiation at ~300°C.

3.2 Dependence of D retention and Li loss on irradiation temperature

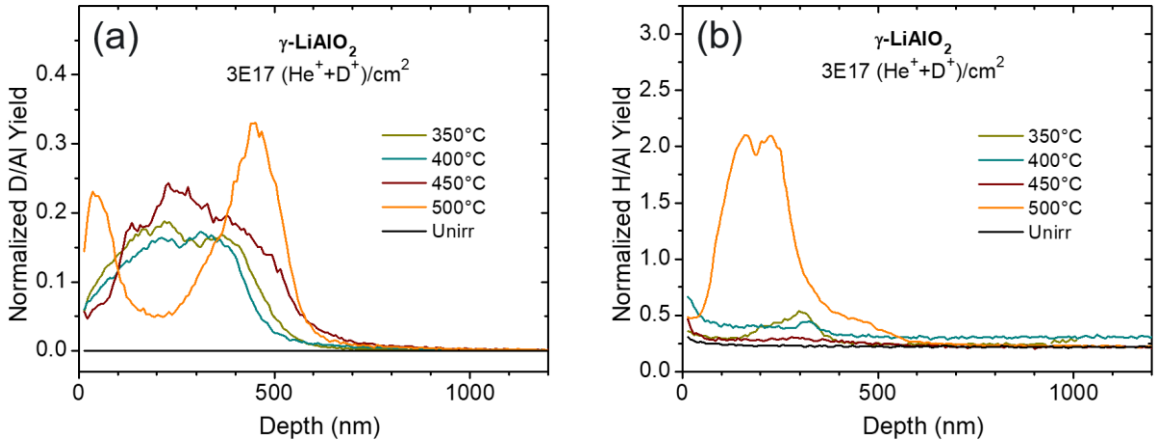

Figure 10. ToF-SIMS depth profiles of normalized (a) D/Al and (b) H/Al yields in γ-$LiAlO_2$ pellets irradiated to 3×10^{17} $(He^+ + D^+)/cm^2$ at various temperatures, along with those in an unirradiated pellet.

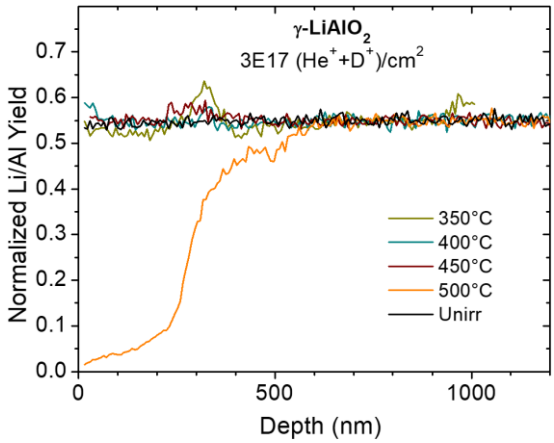

Figure 11. ToF-SIMS depth profiles of normalized Li/Al yields in γ-$LiAlO_2$ pellets irradiated to 3×10^{17} $(He^+ + D^+)/cm^2$ at various temperatures, along with those in an unirradiated pellet.

Figure 10 shows the normalized ToF-SIMS depth profiles of D and H relative to Al yields in the γ-$LiAlO_2$ pellets irradiated to 3×10^{17} $(He^+ + D^+)/cm^2$ at temperatures ranging from 350°C to 500°C. The profiles for an unirradiated pellet are also included for comparison, revealing nearly zero-level D/Al and very low H/Al yields. It is assumed that Al yields remain largely unchanged throughout the depth during ion irradiation. A double-peak structure is observed in the D depth profile at 500°C, as shown in Figure 10(a), with a corresponding H peak at the same depth in Figure 10(b). This pattern is attributed to the isotope exchange between D and H, a phenomenon previously observed in our sequential ion irradiation

studies of γ-$LiAlO_2$ pellets [2]. Isotope exchange is a reversible chemical reaction that transfers isotopes between ions and molecules with no energy difference. This process has been reported to enhance tritium release during neutron irradiation through isotope exchange between H and T [12]. In contrast, the D depth profiles at irradiation temperatures of 450°C and below exhibit single peaks, indicating that isotope exchange is either absent or not detectable under these conditions.

Figure 11 illustrates the normalized Li/Al yields as a function of depth in γ-$LiAlO_2$ pellets irradiated to 3×10^{17} $(He^+ + D^+)/cm^2$ at temperatures ranging from 350°C to 500°C, along with those in an unirradiated pellet. The results demonstrate significant Li loss from the surface region to a depth of ~200 nm during ion irradiation at 500°C. This is also the region where the H peak and D dip are observed, as shown in Figure 10. This depth region likely corresponds to the surface amorphized layer. Due to the uneven surface of the sample at the micrometer scale, the depth of the crater measured by a stylus profilometer is subject to a large error margin. Similar Li loss behavior was also observed in previous studies of γ-$LiAlO_2$ pellets irradiated at 500°C [4,8]. In contrast, Li loss is not observed in the pellets irradiated at lower temperatures. It is noteworthy that a small Li loss was previously observed in a different batch of γ-$LiAlO_2$ pellets irradiated at 300°C [1]. The reasons for this discrepancy are currently unknown, but differences in irradiation conditions and pellet samples could be contributing factors.

4. Conclusions

γ-$LiAlO_2$ pellets were sequentially irradiated to 3×10^{17} $(He^+ + D^+)/cm^2$ at temperatures ranging from 350°C to 500°C. At 350°C, no precipitates were observed, and the microstructure exhibited cavities and fractures. At 400°C, a thin amorphized layer (~70 nm thick) formed on the surface, with resolvable precipitates appearing around the damage peak. Structural fractures and cavities were also visible. This suggests that the critical temperature for precipitate formation under the irradiation conditions of this study lies between 350°C and 400°C. At 450°C, faceted precipitates and cavities developed in the irradiated region with surface amorphization. The characteristics of the precipitates, including size and density, vary with depth and local dose. In the near-surface region, radiolysis and atomic excitation/ionization are the dominant processes, while elastic collision-induced atomic displacements prevail in the deeper regions around the damage peak. At 500°C, large, faceted precipitates formed, up to 200 nm in size, accompanied by surface amorphization. Additionally, isotope exchange between H and D occurred, and significant Li loss was observed in the near-surface region. The results obtained at 500°C are consistent with our previous observations. At the typical ion flux of 3×10^{13} $(ions/cm^2)/s$, a temperature of 500°C is recommended for sequential irradiation with He^+ and D^+ ions to emulate the microstructural features in γ-$LiAlO_2$ irradiated with a thermalized fission neutron spectrum at ~300°C. Further studies on dose rate effects at an elevated temperature are necessary to gain a deeper understanding of their impact on microstructural evolution and compositional changes in γ-$LiAlO_2$ pellets during ion irradiation.

5. Acknowledgments

This work was supported by Tritium Modernization Program, sponsored by National Nuclear Security Administration, U.S. Department of Energy. Ion irradiation was performed at Texas A&M University. Sample characterizations were conducted at PNNL.

6. References

[1] W. Jiang, S.R. Spurgeon, Z. Zhu, X. Yu, K. Kruska, T. Wang, J. Gigax, L. Shao, D.J. Senor, J. Nucl. Mater. 511 (2018) 1.
[2] W. Jiang, T. Wang, Y. Wang, Z. Zhu, L. Shao, D.J. Senor, J. Nucl. Mater. 538 (2020) 152357.
[3] W. Jiang, W.G. Luscher, T. Wang, Z. Zhu, L. Shao, D.J. Senor, J. Nucl. Mater. 542 (2020) 152532.
[4] W. Jiang, L. Kovarik, Z. Zhu, T. Varga, M.E. Bowden, B.E. Matthews, Z. Hu, L. Shao, D.J Senor, J. Appl. Phys. 131 (2022) 215902.
[5] W. Jiang, L. Kovarik, M. G. Wirth, Z. Hu, L. Shao, A. M. Casella, D. J. Senor, J. Nucl. Mater. 591 (2024) 154925.
[6] W. Jiang, J. Zhang, L. Kovarik, Z. Zhu, L. Price, J. Gigax, E. Castanon, X. Wang, L. Shao, D.J Senor, J. Nucl. Mater. 484 (2017) 374.
[7] S. Dudarev *et al*., J. Nucl. Mater. 455 (2014) 16.
[8] W. Jiang, J. Zhang, D.J. Edwards, N.R. Overman, Z. Zhu, L. Price, J. Gigax, E. Castanon, L. Shao, D.J. Senor, J. Nucl. Mater. 494 (2017) 411.
[9] J.F. Ziegler, J.P. Biearsack, U. Littmark, *The stopping and Range of Ions in Solids* (Pergamon Press, New York, 1985); available at: http://www.SRIM.org/.
[10] H. Tsuchihira, T. Oda, and S. Tanaka, Nucl. Instr. Meth. Phys. Res. B 269 (2011) 1707.
[11] S. Agarwal, Y. Lin, C. Li, R.E. Stoller, S.J. Zinkle, Nucl. Inst. Meth. Phys. Res. B. 503 (2021) 11.
[12] M. Nishikawa, T. Kinjyo, T. Ishizaka, S. Beloglazov, T. Takeishi, M. Enoeda, T. Tanifuji, J. Nucl. Mater. 335 (2004) 70.